PHYSICAL REVIEW B **90**, 081109(R) (2014)

Multi-spin-state dynamics during insulator-metal crossover in $LaCoO_3$

A. Doi,[1] J. Fujioka,[1] T. Fukuda,[2,3] S. Tsutsui,[4] D. Okuyama,[5] Y. Taguchi,[5] T. Arima,[5,6] A. Q. R. Baron,[3,4] and Y. Tokura[1,5]

[1]*Department of Applied Physics, University of Tokyo, Hongo, Tokyo 113-8656, Japan*
[2]*Synchrotron Radiation Research Unit, JAEA/SPring-8, Sayo, Hyogo 679-5148, Japan*
[3]*Materials Dynamics Laboratory, RIKEN SPring-8 Center, Sayo, Hyogo 679-5148, Japan*
[4]*Research and Utilization Division, JASRI/SPring-8, Sayo, Hyogo 679-5198, Japan*
[5]*RIKEN Center for Emergent Matter Science (CEMS), Wako, Saitama 351-0198, Japan*
[6]*Department of Advanced Materials Science, University of Tokyo, Kashiwa 227-8561, Japan*

(Received 16 April 2014; revised manuscript received 26 July 2014; published 18 August 2014)

We have investigated the dynamics of spin-state crossover (SSC) for perovskite $LaCoO_3$ through optical phonons by means of infrared and inelastic x-ray spectroscopy. Upon thermally induced SSC, anomalously dispersionless Co-O bond stretching phonons coupled to the thermally excited spin state have been identified. The enhanced spin-state fluctuation irrespective of the presence of a clear charge gap suggests the emergence of complex spin-state disproportionation involving low-, intermediate-, and high-spin states due to the strong correlation among thermally activated spin states.

DOI: 10.1103/PhysRevB.90.081109 PACS number(s): 71.30.+h, 75.25.Dk, 75.30.Wx

The electronic and structural nanoscale texture in complex materials has received enormous attention in recent decades [1]. In particular, the transition-metal oxides provide a fertile arena to realize the self-organization of correlated electrons originating from the interplay among the charge, spin, and orbital degrees of freedom. For example, a variety of charge, spin, and orbital ordering has been identified in perovskite manganites, which often gives rise to a dramatic change of electronic properties as represented by the colossal magnetoresistance [2,3]. In a broader context, it is now well recognized that the manipulation of charge, spin, and orbital structure is the key to control transport, magnetic, or optical properties for various correlated electron systems.

On the other hand, there is another class of materials with unique electron degree of freedom, i.e., spin-state variability. A well-known example is the perovskite $LaCoO_3$, which shows a spin-state crossover (SSC) in the course of thermally induced insulator-metal crossover. In this system, the nominally trivalent Co ion takes three different spin-state configurations: the low-spin (LS) state with filled $3d$ t_{2g} manifold ($S = 0$), intermediate-spin (IS) state with active e_g and t_{2g} orbital degrees of freedom ($S = 1$), and high-spin (HS) state with active t_{2g} orbital degree of freedom ($S = 2$), as shown in Fig. 1(a). At temperatures below 50 K, $LaCoO_3$ is a nonmagnetic insulator, where most of the Co^{3+} ion is in the LS state. Above 100 K, it becomes a paramagnetic semiconductor, showing a hump of the magnetic susceptibility as shown in Fig. 1(b). At higher temperature, it undergoes an insulator-metal crossover between 400 and 600 K, which manifests itself as a moderate reduction of resistivity as seen in Fig. 1(b). Despite the extensive research in recent decades, the dynamics of this enigmatic SSC in the course of insulator-metal crossover, in particular the spin state in the intermediate temperature regime (100 K $< T <$ 500 K), remained still elusive. As a possible model, the uniform IS-state phase with ordering of active e_g orbital is proposed on the basis of *ab initio* calculation, optical spectroscopy, and x-ray diffraction, electron energy loss spectroscopy [4–9]. Another possible scenario is the spatially inhomogeneous spin-state model, i.e., spin-state disproportionation composed of LS and HS states [10–17]. A more complex spin-state disproportionation composed of all the LS, IS, and HS states has also been proposed [14,16,18].

In this Rapid Communication, we have investigated the dynamics of SSC for $LaCoO_3$ through optical phonons by means of inelastic x-ray scattering (IXS) and infrared spectroscopy in a broad temperature range from 10 to 650 K. Anomalously dispersionless Co-O stretching phonons, which are strongly tied with the thermally activated spin states of the Co ion, are identified in the paramagnetic state on the verge of insulator-metal crossover, suggesting the dynamical spin-state disproportionation. The fluctuation of the thermally induced IS and/or HS state is steeply enhanced when their population exceeds a threshold value, while there is little change to the spectral feature of the charge gap. This suggests that the thermally induced spin states undergo large modifications when their density is enhanced; the LS/HS- or LS/IS-state disproportionation is realized at low temperatures with dilute HS- (or IS-) state density, while the complex spin-state disproportionation including all the LS, IS, and HS states emerges at high temperatures on the verge of insulator-metal crossover.

Single crystals of $LaCoO_3$ were grown by the floating-zone method. Magnetization measurements were performed by utilizing a commercial superconducting quantum interference device magnetometer. The spectra of optical conductivity and those of dielectric constant were obtained by Kramers-Kronig analysis of reflectivity spectra. The reflectivity spectra were measured by a Fourier transform infrared spectrometer (0.005–0.7 eV) and a grating spectrometer (0.7–5 eV). The spectra in a vacuum ultraviolet region (5–30 eV) was measured at UV-SOR, Japan. IXS was performed at beam line 35XU [19], SPring-8, Japan. The data were collected using the Si (9 9 9) reflection at 17.794 keV. The typical momentum resolution, ΔQ, is (0.02 0.05 0.05) reciprocal lattice unit.

The optical conductivity spectra for $LaCoO_3$ at various temperatures in the photon energy range of 0–2.5 eV are shown in Fig. 1(c). At 10 K, a charge gap of about 0.3 eV is identified. With increasing temperature, the spectral weight in the low-energy region monotonically increases and the charge

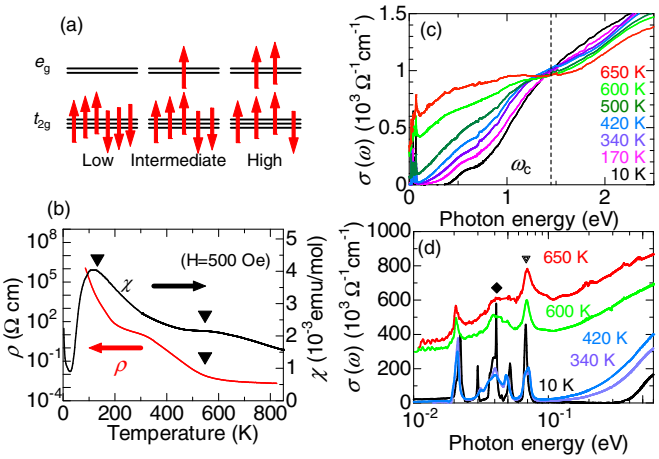

FIG. 1. (Color online) (a) Schematic view of the spin states of trivalent Co ion (Co^{3+}). (b) Temperature dependence of resistivity (ρ) and magnetic susceptibility (χ) for $LaCoO_3$. (c) Temperature variation of the optical conductivity spectra for $LaCoO_3$. (d) The magnified view of the optical conductivity spectra below 0.6 eV. The spectra are plotted on a logarithmic scale in energy. The diamond and doubled triangle indicate the Co-O bond bending mode and Co-O bond stretching modes, respectively.

gap is no longer discernible above 500 K. At high temperatures, the spectral shape is flat aside from the sharp peaks of optical phonons below 0.1 eV, indicating the incoherent charge transport as often observed in correlated metals. Figure 1(d) shows the magnified view of spectra below 0.6 eV. At 650 K, three peak structures are identified at 20, 40, and 69 meV, respectively. According to Ref. [5], the peaks at 40 and 69 meV are assigned to the Co-O bond bending mode and Co-O bond stretching mode, respectively. At low temperatures, the width of each peak decreases and additional peaks are discernible at 30 and 51 meV, respectively.

To get further insight, we have investigated the optical phonons in a wide range of momentum space, in particular focusing on the Co-O bond stretching phonons. Figure 2(a) shows the IXS spectra at (1.74 2.75 0.32) measured at 10 and 280 K. Here, the reciprocal vector is denoted in the representation of pseudocubic unit cell setting. Several optical phonons assigned to the CoO_6-rotational vibration, La-sublattice vibration, and Co-O bond bending/stretching modes [5,7,20] are discernible. Figure 2(b) shows the magnified view of spectra near (1.74 2.75 q) for several q. At 10 K, the antisymmetric Co-O bond stretching (quadrupolar) mode and symmetric (breathing) mode are observed around 72 and 85 meV, respectively. At 280 K, these modes shift in energy to 71 and 82 meV, respectively. In addition, we have observed an additional peak around 68 meV, assigned to the quadrupolar mode activated by the thermally induced HS and/or IS states [7,20]. Such additional modes are observed in the wide range of reciprocal lattice space indicated in Fig. 3(d). For example, the spectra along (1.54 2.54 q) as shown in Fig. 2(c), exhibit the infrared active Co-O bond stretching mode, quadrupolar mode, and breathing mode around 67, 73, and 80 meV, respectively, at 10 K. At 280 K, these modes shift in energy to 64, 69, and 80 meV, respectively. The peak around 73 meV can be assigned

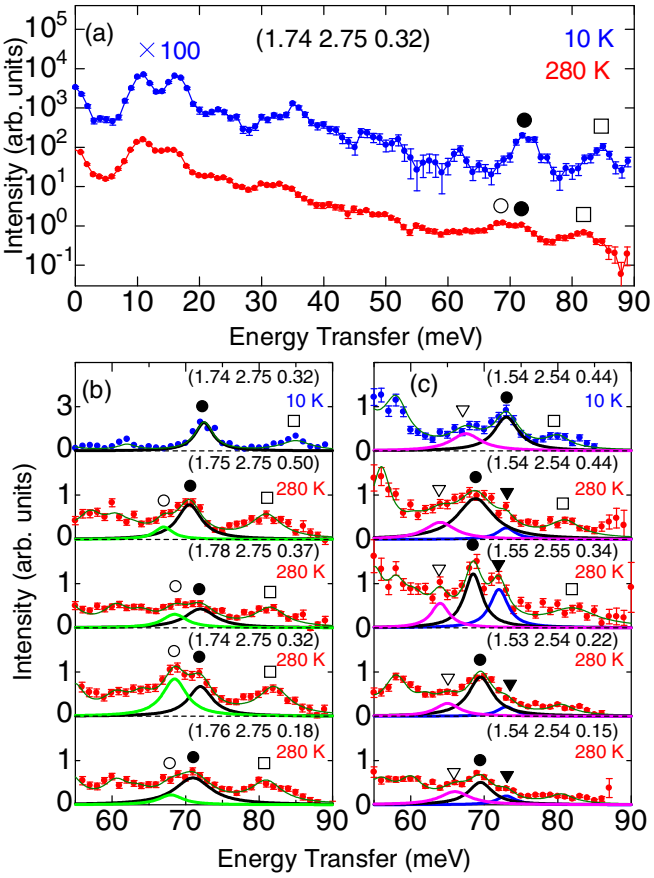

FIG. 2. (Color online) (a) Inelastic x-ray scattering spectra at 10 and 280 K. The 10 K spectrum is scaled 100 times for clarity. Peaks below 25 meV are assigned to CoO_6-rotational vibration, La-sublattice vibration, and accoustic modes, while those between 25 and 60 meV are assigned to Co-O bond bending modes. ● and ○ indicate quadrupolar modes coupled to the LS state and the IS state (or HS state), respectively. □ indicates the breathing mode. Magnified view of spectra between 55 and 90 meV (b) along (1.75 2.75 q) and (c) along (1.54 2.54 q). ▽ and ▼ indicate the infrared active Co-O bond stretching mode coupled to the LS state and the HS state (or IS state), respectively. The background from the elastic scattering and phonons in the low-energy region are subtracted.

to the infrared active Co-O bond stretching mode activated by the thermally induced HS and/or IS states [5].

It is to be noted that such a small dispersion of quadrupolar mode in the wide reciprocal space range is rare among e_g-electron systems with active orbital degree of freedom. For example, in perovskite $La_{1-x}Sr_xMnO_3$, which is characterized by the partially filled e_g band and rhombohedral crystal symmetry comparable with the present system, the dispersion of quadrupolar phonon is as large as 20 meV [21]. This is much larger than the prediction by the shell model calculation on the basis of the repulsive short range interaction and is attributed to a softening (Kohn anomaly) due to the dynamical Jahn-Teller (JT) distortion coupled to the fluctuation of e_g orbital ordering [21]. In this context, the dispersionless quadrupolar mode in the present system suggests that the cooperative JT distortion or instability of e_g orbital ordering, which would be expected in the uniform IS-state phase, is absent. Another more plausible

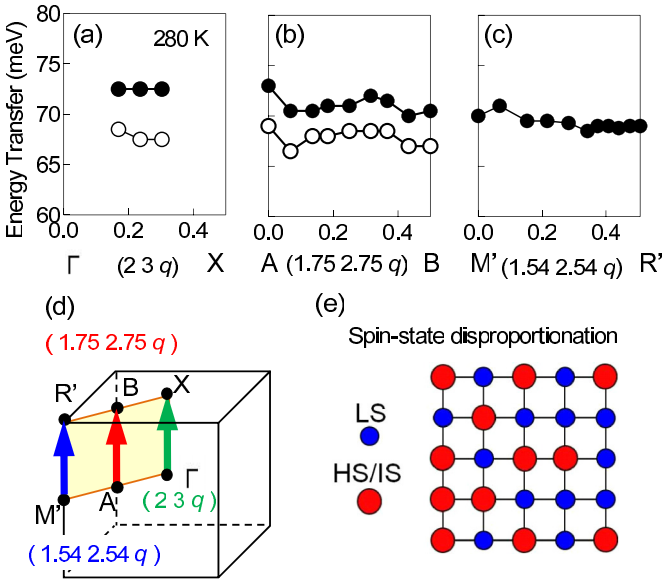

FIG. 3. (Color online) Dispersions of quadrupolar mode along (a) (2 3 q), (b) (1.75 2.75 q), and (c) (1.54 2.54 q) at 280 K. • and ○ indicate the dispersion of quadrupolar mode coupled to the LS state and the HS state (or IS state), respectively. (d) Schematic view of measured points in reciprocal space. The green, red, and blue arrows represent (2 3 q), (1.75 2.75 q), and (1.54 2.54 q), respectively. (e) Schematic view of dynamical spin-state disproportionation.

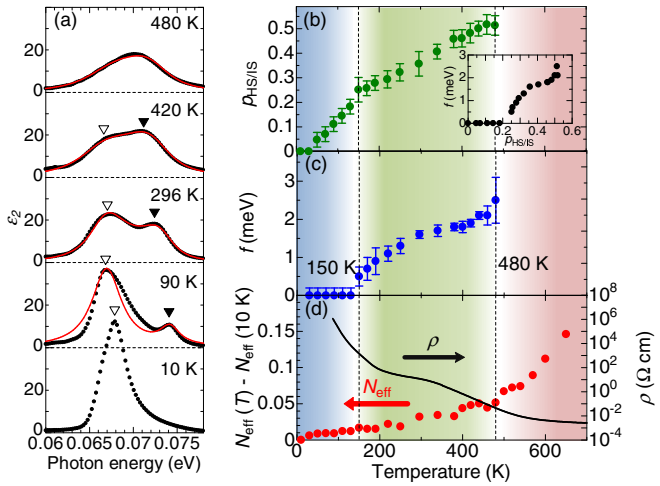

FIG. 4. (Color online) (a) Energy spectra of the imaginary part of the dielectric constant (ϵ_2) around 70 meV. The backgrounds from electronic excitations are subtracted. The open (closed) triangles indicate the Co-O bond stretching mode coupled to the LS state (HS and/or IS state), respectively. Solid red lines denote the best-fitted results by a stochastic analysis of exchange narrowing. The respective spectra are vertically offset by 40 of ϵ_2 for clarity. Temperature dependence of (b) population of the HS state or the IS state ($p_{\mathrm{HS/IS}}$) and (c) fluctuation energy f. (d) Spectral intensity (N_{eff}) and resistivity. The inset to (b) shows f plotted as a function of $p_{\mathrm{HS/IS}}$. The uncertainty in the fitting procedure is represented as an error bar.

scenario is the dynamical spin-state disproportionation [14–16]; two or three different spin states are fluctuating as schematically shown in Fig. 3(e). Since the IS state and/or HS state, are randomly surrounded by a JT-inert LS-state site, the instability of the orbital ordering may be suppressed. Thus, the observed dispersionless quadrupolar phonon in wide range of reciprocal space supports the spin-state disproportionation scenario rather than the uniform IS state with ordering of the e_{g} orbital.

Due to the limitation of energy resolution, it is difficult to analyze more fine structure of phonons on the basis of IXS spectra. To see the evolution of the Co-O stretching mode upon the insulator-metal crossover more precisely, we analyze the spectral shape of the Co-O bond stretching phonons in the infrared spectra in the context of a stochastic theory of exchange (motional) narrowing. According to the conventional mechanism of the exchange narrowing [22], the energy scale of mode splitting and that of fluctuation determines the persistence or amalgamation of two modes; the rapid (slow) fluctuation relative to the mode splitting energy promotes the amalgamation (persistence) of the double-peak structure. According to Ref. [23], when the fluctuation energy between the two states is given by f, the spectral shape of the absorption peak is given by

$$I(\omega) \propto \mathrm{Re}[(q + 2f + i\alpha x)/(q^2 + \alpha^2 + 2qf - 2i\alpha f x)]. \quad (1)$$

Here, $\alpha = \beta - i\gamma/2, \beta = (\omega_{\mathrm{HS/IS}} - \omega_{\mathrm{LS}})/2, \gamma = (\Gamma_{\mathrm{HS/IS}} - \Gamma_{\mathrm{LS}})/2, q = -i(\omega - \omega_0) + \Gamma_0/2, \omega_0 = (\omega_{\mathrm{LS}} + \omega_{\mathrm{HS/IS}})/2$, $\Gamma_0 = (\Gamma_{\mathrm{LS}} + \Gamma_{\mathrm{HS/IS}})/2$, and $x = p_{\mathrm{LS}} - p_{\mathrm{HS/IS}}$. ω_{LS} ($\omega_{\mathrm{HS/IS}}$), Γ_{LS} ($\Gamma_{\mathrm{HS/IS}}$), and p_{LS} ($p_{\mathrm{HS/IS}}$) are the resonance energy, damping constant, and population of the LS state (HS state or IS state), respectively. Figure 4(a) shows the infrared active Co-O bond stretching phonons in the spectra of the imaginary part of the dielectric constant (ϵ_2) and best-fitted results for them (red solid lines). The population of the HS state and/or the IS state ($p_{\mathrm{HS/IS}}$) is plotted as a function of temperature in Fig. 4(b). As temperature increases, $p_{\mathrm{HS/IS}}$ steeply increases above 50 K and reaches around 0.5 at 480 K. The temperature dependence of fluctuation energy f is shown in Fig. 4(c). f abruptly increases above 150 K with the increase of temperature. In the correlated metallic regime above 500 K, f is too large to be captured by the present analysis, or equivalently, the spin state appears to be nearly homogeneous in the time scale of the inverse of a few meV. It is noted that the onset temperature of $p_{\mathrm{HS/IS}}$ is slightly lower than that of f. This difference is more evident in the plot of f as a function of $p_{\mathrm{HS/IS}}$ as shown in the inset of Fig. 4(b). The f steeply increases when $p_{\mathrm{HS/IS}}$ exceeds around 0.2. This means that the fluctuation is slow in the low-temperature regime with dilute HS-state or IS-state sites, while it is enhanced in the intermediate regime with the moderate population of thermally activated spin states.

One possible origin for the enhancement of spin-state fluctuation may be the charge fluctuation associated with the thermally induced insulator-metal crossover. To clarify this possibility, we plotted the temperature dependence of the effective number of electron (N_{eff}) as a measure of the kinetic energy of electrons below ω_c in Fig. 4(d). Here, N_{eff} is defined

as

$$N_{\rm eff}(T) = \frac{2m_0}{\pi e^2 N} \int_0^{\omega_c} \sigma(\omega) d\omega, \qquad (2)$$

where m_0 is the free electron mass, N the number of Co atoms per unit volume, and ω_c the cut-off frequency taken at an isosbestic point [Fig. 1(c)]. $N_{\rm eff}$ smoothly increases as a function of temperature up to 650 K, which contrasts with the steep increase of f and $p_{\rm HS/IS}$. Thus, the onset of f around 150 K may not be directly relevant to the collapse of the charge gap upon the insulator-metal crossover.

Recently, Knížek *et al.* pointed out the emergence of complex spin-state disproportionation upon the insulator-metal crossover [14]. More specifically, when the population of a thermally induced spin state is dilute, the induced state has the character of a HS state, while the character of a IS state becomes prevalent when the population of thermally induced spin-state sites is moderate. They suggest that the complex spin-state interactions among LS, IS, and HS states are essential for such complicated spin-state disproportionation; the repulsive interaction among IS-state sites is weaker than that between HS-state sites. In this context, the enhanced spin-state fluctuation in the intermediate temperature phase may be attributed to the emergence of such a complex spin-state disproportionation, since the dynamical coexistence of the IS state may act as an additional spin-state relaxation channel from the LS state.

In summary, we have investigated the lattice dynamics of the insulator-metal crossover accompanying the spin-state crossover for perovskite $LaCoO_3$ by means of optical and inelastic x-ray spectroscopy. At low temperatures, the quadrupolar phonon, which is strongly coupled to the Co-3d e_g orbitals, exhibits a single peak with an additional peak emerging in the thermally induced paramagnetic state. The momentum dispersion of the thermally induced mode is at most 3 meV in energy width, supporting the spin-state dispropotionation scenario. The frequency of spin-state fluctuation is steeply enhanced when the density of thermally induced spin states exceeds about 20%, while the charge gap exhibits a moderate temperature dependency. This can be explained in terms of the density dependent spin-state disproportionation; a simple LS/HS- or LS/IS-state disproportionation is realized at the initial stage with dilute HS- (or IS-) state density, while the complex spin-state disproportionation involving all of the LS, IS, and HS states is formed when the density of the HS (or IS) state is enhanced. Such a collective spin-state crossover may characterize these classes of correlated electron systems with spin-state variability.

The synchrotron radiation experiments were performed at the BL35XU of SPring-8 with the approval of the Japan Synchrotron Radiation Research Institute (JASRI) (Proposals No. 2012A1250 and 2012B1125). This work was partly supported by JSPS Grant-in-Aid for Scientific Research(S) No. 24224009, and by Funding Program for World-Leading Innovation RUD on Science and Technology (FIRST Program) on Quantum Science on Strong Correlation initiated by the Council for Science and Technology Policy, Japan.

[1] E. Dagotto, Science **309**, 257 (2005).
[2] Y. Tokura, Rep. Prog. Phys. **69**, 797 (2006).
[3] A. Moreo, Science **283**, 2034 (1999).
[4] M. A. Korotin, S. Yu. Ezhov, I. V. Solovyev, V. I. Anisimov, D. I. Khomskii, and G. A. Sawatzky, Phys. Rev. B **54**, 5309 (1996).
[5] S. Yamaguchi, Y. Okimoto, and Y. Tokura, Phys. Rev. B **55**, R8666 (1997).
[6] G. Maris, Y. Ren, V. Volotchaev, C. Zobel, T. Lorenz, and T. T. M. Palstra, Phys. Rev. B **67**, 224423 (2003).
[7] A. Ishikawa, J. Nohara, and S. Sugai, Phys. Rev. Lett. **93**, 136401 (2004).
[8] K. Knížek, P. Novák, and Z. Jirák, Phys. Rev. B **71**, 054420 (2005).
[9] R. F. Klie, J. C. Zheng, Y. Zhu, M. Varela, J. Wu, and C. Leighton, Phys. Rev. Lett. **99**, 047203 (2007).
[10] P. M. Raccah and J. B. Goodenough, Phys. Rev. **155**, 932 (1967).
[11] P. G. Radaelli and S.-W. Cheong, Phys. Rev. B **66**, 094408 (2002).
[12] Y. Kobayashi, T. S. Naing, M. Suzuki, M. Akimitsu, K. Asai, K. Yamada, J. Akimitsu, P. Manuel, J. M. Tranquada, and G. Shirane, Phys. Rev. B **72**, 174405 (2005).
[13] M. W. Haverkort *et al.*, Phys. Rev. Lett. **97**, 176405 (2006).
[14] K. Knížek, Z. Jirák, J. Hejtmánek, P. Novák, and W. Ku, Phys. Rev. B **79**, 014430 (2009).
[15] J. Kuneš and V. Křápek, Phys. Rev. Lett. **106**, 256401 (2011).
[16] V. Křápek, P. Novák, J. Kuneš, D. Novoselov, Dm. M. Korotin, and V. I. Anisimov, Phys. Rev. B **86**, 195104 (2012).
[17] G. Zhang, E. Gorelov, E. Koch, and E. Pavarini, Phys. Rev. B **86**, 184413 (2012).
[18] K. Asai, A. Yoneda, O. Yokokura, J. M. Tranquada, G. Shirane, and K. Kohn, J. Phys. Soc. Jpn. **67**, 290 (1998).
[19] A. Q. R. Baron, Y. Tanaka, S. Goto, K. Takeshita, T. Matsushita, and T. Ishikawa, J. Phys. Chem. Solids **61**, 461 (2000).
[20] N. O. Golosova, D. P. Kozlenko, A. I. Kolesnikov, V. Y. Kazimirov, M. B. Smirnov, Z. Jirák, and B. N. Savenko, Phys. Rev. B **83**, 214305 (2011).
[21] W. Reichardt and M. Braden, Physica (Amsterdam) **263-264**, 416 (1999).
[22] A. Abragam, *The Principles of Nuclear Magnetism* (Clarendon, Oxford, 1962).
[23] M. Tanaka, K. Siratori, and N. Kimizuka, J. Phys. Soc. Jpn. **53**, 760 (1984).